Preparation of functionalized Ayous sawdust-carbon nanotubes composite for the electrochemical determination of carbendazim pesticide

Ghislaine Ariane Fozing Mekeuo, Christelle Despas, Charles Péguy Nanseu-Njiki, Alain Walcarius, Emmanuel Ngameni

Preparation of functionalized *Ayous* sawdust-carbon nanotubes composite for the electrochemical determination of carbendazim pesticide

Ghislaine Ariane Fozing Mekeuo,[a,b] *Christelle Despas,*[b,*] *Charles Péguy Nanseu-Njiki,*[a] *Alain Walcarius*[b] *and Emmanuel Ngameni*[a,*]

[a] Laboratoire de Chimie Analytique, Faculté des Sciences, Université de Yaoundé I, BP 812 Yaoundé, Cameroun
[b] Université de Lorraine, CNRS, LCPME, F-54000 Nancy, France
* E-mail: christelle.despas@univ-lorraine.fr, engameni@yahoo.fr

Received: ((will be filled in by the editorial staff))
Accepted: ((will be filled in by the editorial staff))

Abstract
Fine particles of *Ayous* sawdust (AS) were successfully modified by maleic anhydride to increase their accumulation capability towards carbendazim (Cbz) and used to modify glassy carbon electrode (GCE) for the detection of this pesticide. For a more efficient use of the biosourced material as electrode modifier for electrochemical detection, the functionalized particles were mixed with carbon nanotubes to yield a conductive composite. After characterization by cyclic voltammetry and electrochemical impedance spectroscopy, the modified GCE was applied to Cbz detection. A sensitivity of (2.61 ± 0.08) μA M^{-1} and a detection limit of 0.04 μM were determined under optimized experimental conditions. Moreover, the designed sensor was found efficient for Cbz determination in real samples (spring water and commercial pesticide product).

Keywords: *Ayous* sawdust, maleic anhydride, carbon nanotubes, carbendazim, electrochemical detection

DOI: 10.1002/elan.((will be filled in by the editorial sttaff))

1. Introduction

Conventional working electrodes used as amperometric sensors present relatively poor performance, due to the lack of selectivity and/or low sensitivity [1]. Among the various strategies used to circumvent these drawbacks, the use of materials deposited as thin films on the electrodes surface is widely applied [2]. Several materials are commonly used as electrode modifiers, such as clay minerals [3-6], mesoporous (organo)silica [7], zeolites [8] and synthetic or natural polymers [9].

Lignocellulosic materials (LMs), abundant and cheap wastes from agricultural, forestry and industrial activities have shown attractive sorption properties that explain their growing use for the removal of pollutants. LMs possess valuable cation exchange capacity likely to be exploited for the immobilization of heavy metals [10-13]. The organic character of their building blocks that consist in varying proportions of cellulose, hemicelluloses and lignin [14, 15], enables the adsorption of many harmful organic compounds such as dyes and pesticides [10, 16]. However, LMs are still poorly used as electrode modifier despite their availability, their sorption capability and the well-known experimental approaches to combine the chemistry of insulator materials with electrochemistry (*i.e.*, deposition as thin films on conductive surface or incorporation into a conductive matrix (*e.g.*, carbon paste [3, 7, 8, 17])).

Ayous (*Triphochiton Schleroxylon*) sawdust is an abundant waste from West and Central Africa wood Industry. Several works report the use of this material as efficient adsorbent of heavy metals [18-21] and pesticide [22, 23]. Recently, Dedzo et al. showed that *Ayous* sawdust can be deposited as thin film onto glassy carbon electrode and the resulting sensor used for the amperometric determination of paraquat [24]. Surface treatments of this LM or its use as component in composite material are likely to enhance further its properties. Recently, an alginate-*Ayous* sawdust composite has proven to be low-cost material for the removal of Cd(II) [25]. Njine-Bememba et al. demonstrated that amine functionalized *Ayous* sawdust can adsorb anions, which is not the case for the unmodified ones [26]. More recently, Ngana et al. improved Pb(II) electrochemical detection with a dye functionalized *Ayous* sawdust modified electrode [27]. The insulating character of *Ayous* sawdust could however restrict its use as electrode modifier. A strategy to circumvent this limitation is its association to conductive nanomaterials to obtain a conductive composite.

Carbon nanotubes (CNTs) are particularly attractive electrode modifiers because of their large surface area,

high electrical conductivity and electrocatalytic properties that improve the electrochemical signal of various target analytes, leading to both higher sensitivity and better selectivity. The corresponding CNT-modified electrodes are prepared according to various strategies such as CNTs dispersion in different binders, drop coating on solid electrodes, screen printing, formation of composites or CNTs attachment by abrasion [28-30]. Their tendency to form aggregates in several solvents, due to strong organophilic interactions [31], needs to be taken into accounts when preparing thin films on electrode surfaces, for which a good dispersion of CNTs is required [29].

Carbendazim (methyl benzimidazol-2-ylcarbamate, Cbz) is a toxic class IV systemic fungicide that belongs to benzimidazole chemical group. It can be used to control a wide range of fungal diseases [32-34]. Classified as hazardous chemical by World Health Organization, Cbz is identified as possible human carcinogens [35]. Spectrophotometry [36, 37], chromatography [38, 39] and spectrofluorimetry [40, 41] are analytical methods frequently used for its determination. Despite their high accuracy and sensitivity, these methods are expensive, require sophisticated instrumentation and sample preparation (involving several time-consuming steps). By contrast, electrochemical methods offer certain advantages such as low cost of instrumentation, fast analysis and high sensitivity [42, 43]. Recently, electrochemical methods based on various electrode modifiers have been reported for the electrochemical determination of carbendazim in various matrices [44-57]. To the best of our knowledge, sawdust-CNTs composite material is not yet reported as electrode modifier for Cbz determination.

The objective of this work is to design and evaluate a new electrochemical sensor based on lignocellulosic material for pesticide analysis. For this purpose, maleic anhydride (MA) was grafted on *Ayous* sawdust (AS) and the resulting material mixed with carbon nanotubes (CNTs) to prepare a conductive composite, in order to improve the performance of the resulting amperometric sensor by enhancing both the sorption capability and the electron transfer process. After characterization of the synthesized materials by Fourier-Transform InfraRed (FTIR) spectroscopy and Scanning Electron Microscopy (SEM), cyclic voltammetry (CV) and electrochemical impedance spectroscopy (EIS) were performed to evaluate the electrochemical response of the modified electrodes using selected redox probes. The effect of the amount of sawdust within the composite was particularly investigated. Subsequently, these electrodes were applied for the detection of carbendazim (Cbz) in aqueous solution, in spring water and in a commercial formulation.

2- Experimental section

2-1- Materials, chemicals and reagents

Ayous sawdust (AS) was collected in a sawmill (Yaoundé (Cameroon) and the fine fraction (particle diameter < 5µm), isolated by gravimetry [24], used in this work.

Carbendazim ($C_9H_9N_3O_2$, 97%), polyvinylpyrrolidone (PVP) (M 10000 g mol^{-1}), carbon nanotubes (CNTs, 90%, D×L 110-170 nm × 5-9µm) and maleic anhydride (MA, $C_4H_2O_3$, 99%) were purchased from Sigma Aldrich. All other chemicals were analytical grade: sodium hydrogen phosphate (Na_2HPO_4, 98%, Aldrich), sodium dihydrogen phosphate (NaH_2PO_4, 98%, Aldrich), potassium hydroxide (KOH), hydrochloric acid (HCl), potassium bromide (KBr, 99%, PIKE), aluminium sulfate ($Al_3(SO_4)_2$, 98%, Prolabo), calcium chloride ($CaCl_2$, 80%, Labosi), iron (III) sulfate ($Fe_2(SO_4)_3$, 98%, Prolabo), magnesium sulfate ($MgSO_4$, 99%, Prolabo), and copper (II) sulfate pentahydrate ($CuSO_4.5H_2O$, 98%, Acros - Organics).

Ruthenium hexamine chloride ($Ru(NH_3)_6Cl_3$, 98%, Aldrich), potassium hexacyanoferrate (III) ($K_3Fe(CN)_6$, 98%, Prolabo) and potassium chloride (KCl, 99%, Prolabo) were used respectively as redox probe and supporting electrolyte for the electrochemical characterization of the modified glassy carbon electrodes. The ionic liquid, 1-butyl-3-methylimidazolium chloride (BMIMCl), was synthesized according to the literature [58] using 1-methylimidazole (99%) and 1-chlorobutane (99.5%) purchased from Sigma Aldrich.

All solutions were prepared using deionized water (18 MΩ cm). Spring water samples were collected near Mendong-Yaoundé city. The samples were first filtered using Whatman filter papers grade 40 and centrifuged in order to remove suspended solids. Some physicochemical characteristics of this spring water (pH 4.9, conductivity 2.19 µS.cm^{-1} and turbidity 185 NFU) were determined prior to the electrochemical experiments.

2-2- Modification of *Ayous* sawdust by maleic anhydride

Some previous studies showed that ionic liquids (ILs) are suitable solvents for homogeneous functionalization of LMs without the need of catalysts and under mild conditions [59-61]. Here, BMIMCl acts as a swelling agent by reducing the strength of the hydrogen bond network of cellulose and therefore promoting the diffusion of the modifier and the exposition of alcohol moieties for functionalization [62-65]. In practice, 0.17 g of *Ayous* sawdust was dispersed in 4 g of BMIMCl pre-heated at 120 °C and stirred vigorously for 30 min under argon

atmosphere. Maleic anhydride (0.7 g) was then added and the mixture stirred for 4 hours. The solid residue was washed several times with deionized water and centrifuged (5 × 50 mL). Finally, the material was dried for 48 hours at room temperature and at 105°C for 2 hours. The dried maleic anhydride modified *Ayous* sawdust (named MAS) was stored in a sealed vial.

2-3- Preparation of *Ayous*-CNTs-based composite films on carbon electrodes

Before electrochemical measurements, the surface of the glassy carbon electrode (GCE) was polished (alumina slurry, 0.05 µm particles), rinsed with deionized water, sonicated for 5 min and finally rinsed once again with deionized water.

For the electrode modification by AS or MAS, 5µL of an aqueous suspension of these materials (2 g L^{-1}) was carefully deposited at the surface of the GCE electrode. The film was dried at ambient temperature for 2 hours and the modified electrodes (respectively named GCE/AS and GCE/MAS) used without any further pre-treatment.

For the carbon composite modified electrodes, CNTs and PVP (chosen as dispersant [66-68]), were mixed in water to obtain concentrations of 2 g L^{-1} and 0.02 g L^{-1}, respectively. Subsequently, AS or MAS was introduced to obtain concentrations of 0.05 g L^{-1}, 0.1 g L^{-1}, 0.2 g $L^{-1}$and 0.5 g L^{-1}. These concentrations correspond to AS or MAS mass percentages relative to CNTs of 2.4%, 4.8%, 9% and 20%, respectively. As the control sample, a suspension with only CNTs (2 g L^{-1}) and PVP (0.02 g L^{-1}) was also prepared. All the mixtures were sonicated for 4 hours to obtain a stable dispersion. The film deposition onto GCE electrode followed the same procedure as described above. The obtained electrodes were denoted GCE/CNTs-AS_x or GCE/CNTs-MAS_x, where x represents the mass percentages of AS or MAS relative to CNTs. The electrode modified by CNTs was denoted GCE/CNTs.

2-4- Instrumentation

The modified and unmodified electrodes were used in a standard three electrodes electrochemical cell. A saturated calomel electrode was used as reference and a platinum wire as counter electrode. These electrodes were connected to a µ-Autolab potentiostat controlled by the GPES (General Purpose Electrochemical System) software.

Cyclic voltammetry (CV) was used for electrochemical characterization and the study of the electrochemical behaviour of carbendazim. Differential pulse voltammetry (DPV) was used for quantitative analyses of pesticide, using the following parameters: modulation time 0.05 s, interval time 0.1 s, step potential 0.05 $V.s^{-1}$ and modulation amplitude 0.5 V. Electrochemical impedance spectroscopy was performed with ferri/ferrocyanide couple (1 mM of each salt) solubilized in 0.1M KCl as electrolytic solution. The frequency range selected was 10 KHz to 10 MHz and the applied potential was relative to the open circuit potential for each electrode, with an amplitude of 10 mV.

FTIR spectra were recorded in transmission mode within the wave number range of 4000 cm^{-1} to 400 cm^{-1} with a resolution of 4 cm^{-1} on an Alpha spectrometer from Bruker Optics. Pellets were prepared by mixing a small amount of wood material with four times of KBr.

SEM micrographs were obtained from a JEOL JCM-6000 apparatus operating at an accelerating voltage of 15 kV.

3-Results and discussions

3-1- Materials characterization

Functionalization of *Ayous* sawdust was first followed by infrared spectroscopy. FTIR spectra of AS before and after modification are presented in Figure 1. Both spectra showed the typical bands of lignocellulosic material [69-73]. The wide band centred at 3340 cm^{-1} was characteristic of the stretching vibrations of the O-H bonds of alcohols and hydrogen-bonded water molecules. The overlapped bands centred at 2943 cm^{-1} were assigned to the aliphatic C-H bonds. The reaction between anhydride molecules and the terminal OH groups of the wood was confirmed by the substantial growth of the C=O band at 1734 cm^{-1} that is consistent with the formation of ester bonds [69-72].

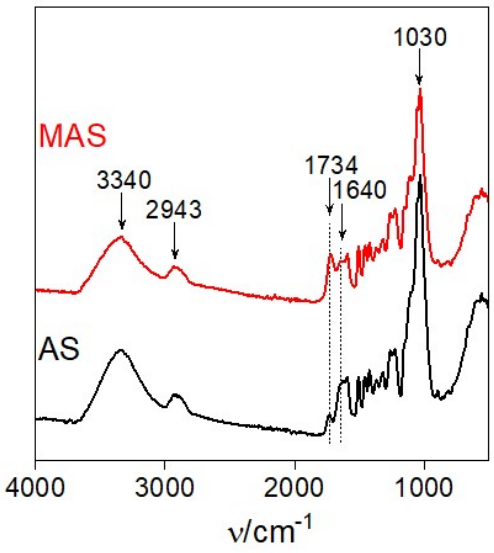

Figure 1. FTIR spectra of pristine (AS) and maleic anhydride modified (MAS) *Ayous* sawdust.

The very intense band at 1030 cm^{-1} was due to the C-O bonds [70]. The high intensity of this band was explained by the abundance of these chemical groups in the constituents of wood (cellulose, hemicelluloses and lignin). Assuming that the grafting reaction occurred mainly on the primary alcohol functions of cellulose, the scheme 1 is proposed.

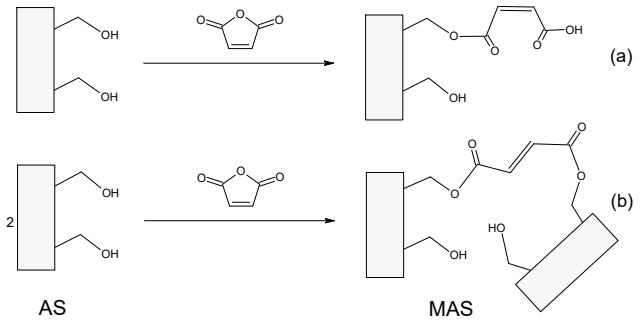

Scheme 1. Proposed reaction mechanism between maleic anhydride and *Ayous* sawdust in BMIMCl. (a) Single grafting and (b) grafting with reticulation.

The morphology of thin films deposited at glassy carbon electrodes (GCE/MAS, GCE/CNTs CNTs-$MAS_{4.8}$ and CNTs-MAS_{20}) were examined by scanning electron microscopy (Figure 2). Maleic anhydride modified Ayous film displayed homogeneous layer of flat and curvy sawdust particles with sizes lower than 10 µm (Fig. 2A). These flat shapes are reminiscent of the cell walls of the cellulosic fiber of wood. The dense network of deposited CNTs was consistent with the high organophilic nature of CNTs and the π-π interactions between adjacent nanotubes (Fig. 2B). In the case of the MAS-CNTs composites (Fig. 2C&D), sawdust particles were dispersed and trapped in the CNTs network.

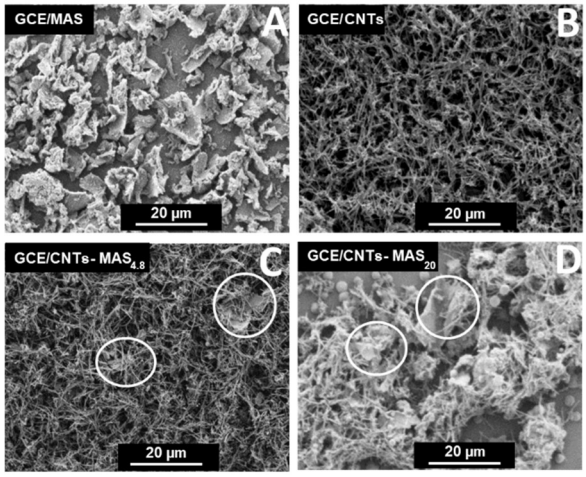

Figure 2. Scanning electron micrographs of GCE covered with (A) MAS, (B) CNTs (C) CNTs-$MAS_{4.8}$ and (D) CNTs-MAS_{20}. White circles highlight LM particles in the composite

3-2- Electrochemical behaviour of the modified electrodes

Electrochemical characterization of the modified electrodes were first performed using model cationic ($Ru(NH_3)_6^{3+}$, Fig. 3A) and anionic ($Fe(CN)_6^{3-}$, Fig. 3B) redox probes in order to evaluate the effect of the modifier on the electrode accessibility.

3-2-1- Electrochemical behaviour of $Ru(NH_3)_6^{3+}$

Multisweep cyclic voltammograms recorded on GCE/MAS in a 0.5 mM $Ru(NH_3)_6^{3+}$solution display a gradual increase of the signals (inset of Fig. 3A) due to the progressive accumulation of cations onto the carboxylate-modified sawdust [24, 26]. The peak current at steady-state was three times more intense than on bare GCE (15.6 µA at GCE/MAS and 5 µA at GCE). MAS film also demonstrated higher accumulation of cations compared to untreated sawdust film (current peak of 10.5 µA at GCE/AS, see Fig. S1A) consistent with carboxylate functions promoted onto the *Ayous* by sawdust following the treatment with maleic anhydride. Note that the signal intensities were stabilized after 30 scans at GCE/AS (Fig S1A) while 100 scans were needed for GCE/MAS (Fig. 3A, Inset). The slower film saturation on GCE/MAS can be explained by the occlusion of the adsorption sites in MAS. This was certainly the consequence of the partial reticulation of sawdust, following the reaction with maleic anhydride (Scheme 1(b)). Such reticulation can promote the formation of smaller pores, making slower the diffusion of $Ru(NH_3)_6^{3+}$ species through the film.

When MAS was dispersed in CNTs matrix, $Ru(NH_3)_6^{3+}$ accumulation was still observed (Fig. S1B), evidencing that the biomaterial still kept its cation accumulation properties in the composite material. The less intense signal was explained by the lesser amount of MAS present on the electrode surface in the case of GCE/CNTs-MAS_{20} compared to GCE/MAS (see section 2.3). Similar behaviour was observed when AS was used for the preparation of the composite (*i.e.*, GCE/CNTs-AS_{20}). However, the saturation of the composite by $Ru(NH_3)_6^{3+}$ cations was much faster (Fig. S2).Almost no accumulation was observed for GCE/CNTs (*i.e.*, in the absence of *Ayous*), resulting in a CV response close to that of bare GCE (see curves d & e in Fig. 3A).

3-2-2- Electrochemical behaviour of $Fe(CN)_6^{3-}$

Because of the negatively charged surface of modified *Ayous* sawdust that induced an electrostatic repulsion effect, the electrochemical response of the $Fe(CN)_6^{3-}$ at GCE/MAS was a poorly defined signal of lower intensity

in comparison to that recorded on bare GCE (curves a and e in Fig. 3B). The peak potential separation (ΔE) was above 300mV, far from the 60 mV expected for a fast monoelectronic redox system. This showed that MAS prevents fast charge and mass transfer kinetics for this probe [24]. After incorporation of MAS in CNTs (i.e. GCE/CNTs-MAS_{20}), a reversible signal was recovered (see curve c in Fig. 3B) thanks to the electrocatalytic properties of carbon nanotubes [74]. The slightly larger currents compared to bare GCE were explained by the large surface area in the presence of CNTs, promoted by the presence of modified *Ayous* particles (Fig. S3).

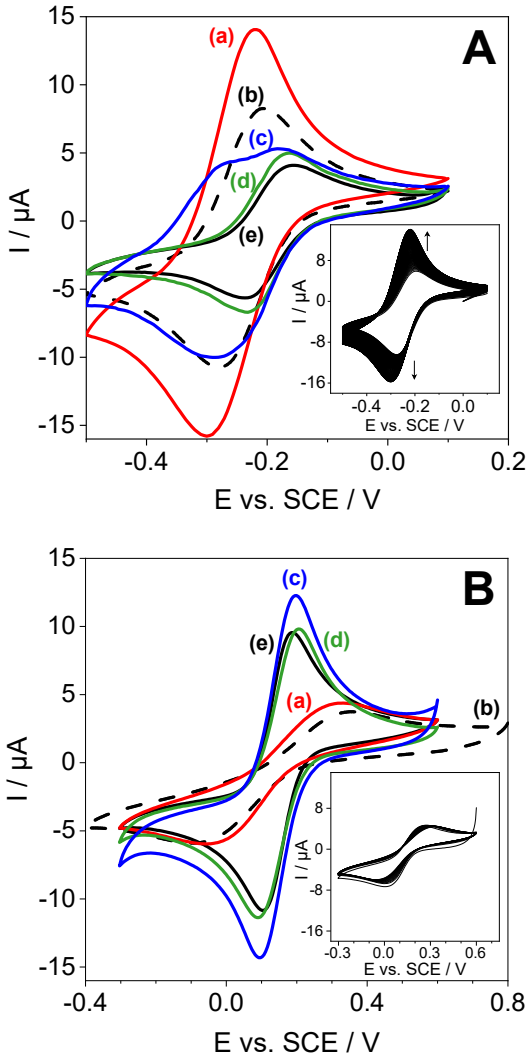

Figure 3. Cyclic voltammograms at steady-state recorded at 50 mV s^{-1} using various working electrodes in (A) 0.5 mM $[Ru(NH_3)_6]^{3+}$ and (B) 1 mM $[Fe(CN)_6]^{3-}$ (in 0.1 M KCl, pH 6.5). Electrodes: (a) GCE/MAS, (b) GCE/AS, (c) GCE/CNTs-MAS_{20}, (d) GCE/CNTs and (e) bare GCE. Insets: multisweep CVs obtained for GCE/MAS with the respective probes.

The Nyquist plots recorded in 0.1M KCl containing 1mM $Fe(CN)_6^{3-}/Fe(CN)_6^{4-}$ on CGE and modified electrodes are shown in Figure 4. These curves present well-defined capacitive loops at high frequency values, assigned to the electron transfer during the electrochemical reaction. The linear part was characteristic of the diffusion process. The charge transfer resistance (R_{CT}) values, characteristic of the kinetics of electron transfer, were obtained from the diameter of these capacitive loops [75]. As expected, the deposition of lignocellulosic materials alone increased dramatically the R_{CT} of the resulting electrodes because of the insulating properties of *Ayous* sawdust particles (R_{CT} of 0.5 kΩ, 86 kΩ and 72 kΩ respectively for GCE, GCE/AS and GCE/MAS). The benefit of the presence of carbon nanotubes in the preparation of the electrode modifier was clearly evidenced by the large decrease of R_{CT} values (*i.e.*, 0.75 kΩ for GCE/CNTs-MAS_{20}). The same tendency was observed for GCE/CNTs-AS_{20} (R_{CT} equal to 0.99 kΩ). These values were *ca.* 1.5-2 times larger than bare GCE, but also two orders of magnitude lower than those observed with electrodes made of only *Ayous* materials. These results confirmed the ability of CNTs to improve electrode conductivity by promoting the electron mobility throughout the composite.

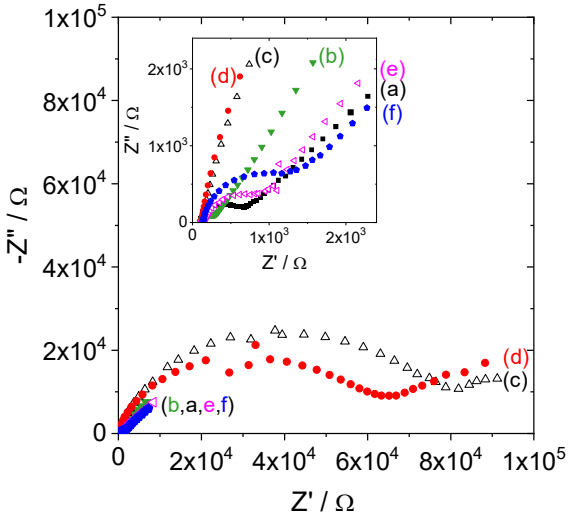

Figure 4. EIS signals recorded in 1 mM $Fe(CN)_6^{3-}$ and $Fe(CN)_6^{4-}$ and 0.1 M KCl solution, in a frequency range from 10 KHz to 10 MHz, using various working electrodes: (a) GCE, (b) GCE/CNTs, (c) GCE/AS, (d) GCE/MAS, (e) GCE/CNTs-AS_{20} and (f) GCE/CNTs-MAS_{20}. Inset depicts an enlarged view of the high frequency region.

3-3- Application to carbendazim electroanalysis

3-3-1- Detection of Cbz at modified electrodes

Figures 5 displays cyclic voltammograms of Cbz (50 µM in phosphate buffer at pH 7) recorded on various electrodes. When using *Ayous* sawdust modified GCE, Cbz undergoes an irreversible oxidation (Fig. 5A), independently on the fact that the LM material has been functionalized with maleide anhydride or not. At bare GCE, two small reduction peaks during the reverse scan. The presence of LMs thin films induced an overvoltage of the oxidation signal due to the insulating character of AS and MAS. The potential shift was however less important at GCE/MAS (+0.09 V) than at GCE/AS (+0.19 V). The treatment of *Ayous* sawdust by maleic anhydride induced a more defined and intense oxidation peak compared to the pristine material. The intensity of the signal at GCE/MAS was enhanced by a factor 1.5 compared to the bare electrode (*i.e.*, 2.3µA and 3.5µA, respectively for GCE and GCE/MAS). The chemical pre-treatment of the *Ayous* sawdust by maleic anhydride thus confers to the material interesting adsorption properties towards Cbz. This is consistent with Cbz adsorption through hydrogen bonding interactions on other carboxylic acid-bearing supports [49].

When the electrodes were modified by CNTs-sawdust composites, some interesting behaviours were observed. The electrochemical response of carbendazim occurred at a less anodic potential, comparable to that of bare GCE. Moreover, a cathodic signal was visible on the reverse scan (see curve c in Fig. 5B). This can be assigned to the electrocatalytic properties of CNTs. For the same concentration of pesticide, the current peak obtained on GCE/CNTs-MAS$_{4.8}$ was about 10 times higher than that recorded on GCE/MAS. It is noteworthy that Cbz can also interact with CNTs [46, 76], but the presence of modified *Ayous* sawdust contribute to enhance the accumulation/detection of the analyte (compare curves c & d in Fig. 5B).

3-3-2- Effect of the amount of Ayous sawdust in the composite on the electrochemical detection of Cbz

The effect of the amount of MAS in the composite (0 to 20% with respect to CNTs) on the performance of GCE/CNTs-MAS$_x$ was studied. Figure 6A displays the overlay of the first cyclic voltammograms recorded on GCE modified by CNTs-MAS$_x$. By increasing the percentage of modified LM into the composite, the response of the sensor increased up to 4.8%. The current intensities were then found to decrease progressively from 9% to 20% of MAS (see upper part of Fig. 6B). The anodic peak potential shifted to more positive values and the reverse reduction signal tended to disappear as the percentage of MAS was increased (see inset of Fig. 6A and lower part of Fig. 6B). Consistent with EIS results described above, these results can be attributed to the insulating character of Ayous sawdust that slowdown the electron transfer reactions at the composite electrode. Based on variations of peak currents (Fig. 6B), GCE/CNTs-MAS$_{4.8}$ was kept for further Cbz detection experiments.

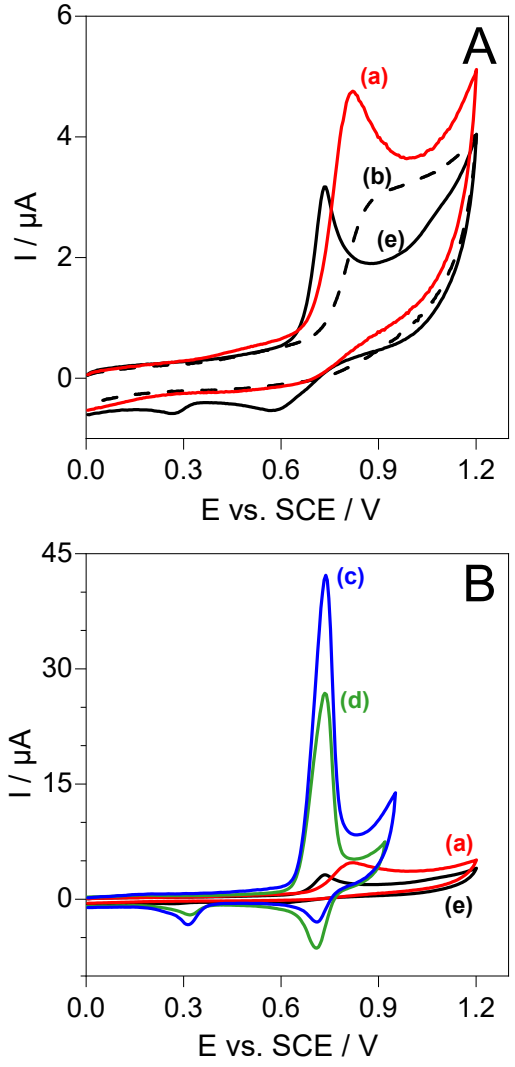

Figure 5. Cyclic voltammograms recorded at 50 mV s^{-1} in a solution containing 50 µM Cbz (in 0.1 M phosphate buffer, pH 7.0) using electrodes prepared in (A) absence and (B) presence of CNTs. Electrodes: (a) GCE/MAS, (b) GCE/AS, (c) GCE/CNTs-MAS$_{4.8}$, (d) GCE/CNTs and (e) bare GCE.

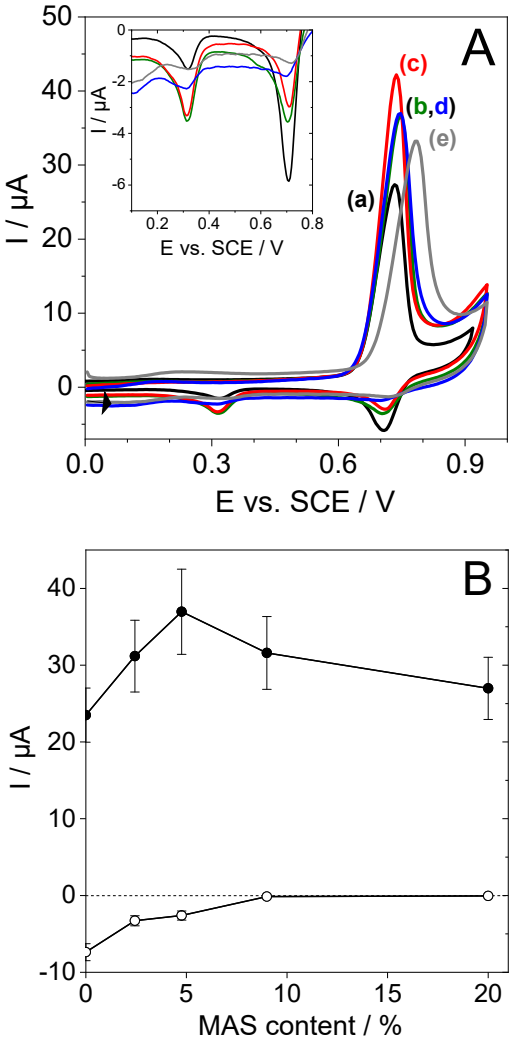

Figure 6. (A) Cyclic voltammograms (first cycles) recorded at 50 mV s^{-1} in a solution containing 50 µM Cbz (in 0.1 M phosphate buffer, pH 7.0) using GCE/CNTs-MAS_x electrodes prepared from various amount of MAS (x%): (a) 0% (b) 2.4%, (c) 4.8%, (d) 9% and (e) 20%; The inset is an enlarged view of the reverse cathodic signals. (B) Variation of peak currents (● oxidation and ○ reduction) as a function of the MAS content in the composite electrodes (error bars correspond to n=5).

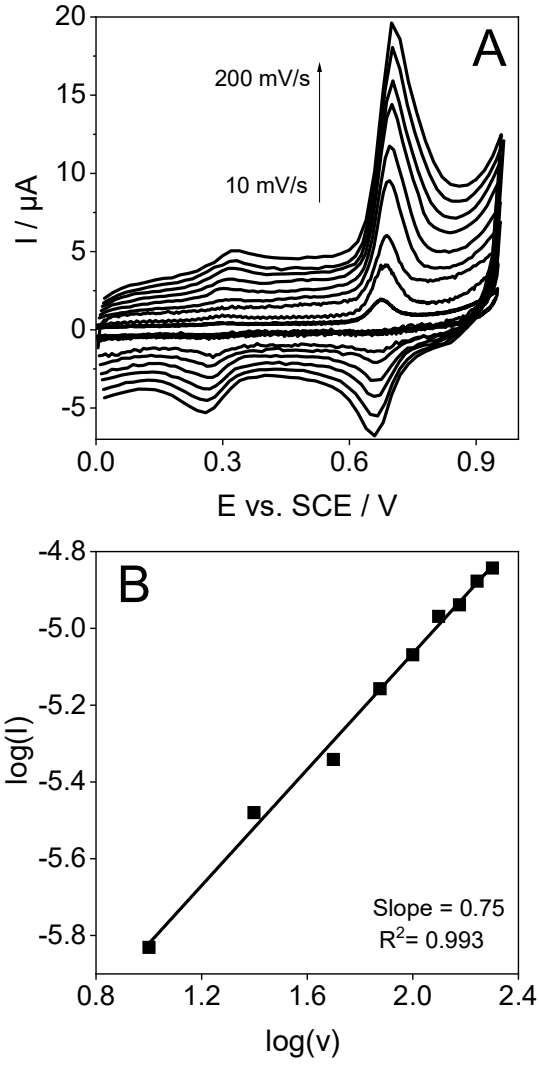

Figure 7. (A) Cyclic voltammograms recorded at various scan rates (10, 25, 50, 75, 100, 125, 150, 175, 200) mV s^{-1} in a solution containing 5 µM Cbz (in 0.1 M phosphate buffer, pH 5.0) using GCE/CNTs-$MAS_{4.8}$. (B) Variation of log(I) for the peak current as a function of log(v) (v = potential scan rate).

3-3-3- Effect of potential scan rate on the voltammetric response of Cbz at GCE/CNTs-$MAS_{4.8}$

The influence of potential scan rate on the electrochemical response of Cbz was studied by CV, as shown in Figure 7. Both anodic and cathodic peak currents increased with the scan rate (Fig. 7A). A double logarithmic plot of anodic peak current versus the potential scan rate yielded a linear trend ($R^2 > 0.99$) with equation $\log ip = 0.755 \times \log v - 6.577$ (Fig. 7B). The slope (0.75) indicated a mixed diffusion and adsorption process. Indeed, a slope of 0.5 indicated a purely diffusion controlled process while a slope of 1.0 was related to an adsorption-based process, and intermediate values a mixed process [76, 77]. This confirms that the composite electrode accumulated Cbz via adsorption and that the electrode reaction process was limited by mass transport through the porous film.

3-3-4- Quantitative analysis of Cbz

Differential pulse voltammetry (DPV) was implemented for the quantitative analysis of Cbz. After investigating the

influence of pH on the DPV response, the calibration curve for optimal conditions was obtained and the method was extended to real case analysis.

Effect of pH. The influence of the pH of the electrolytic solution (in the range 3 to 11) on the oxidation signal of 50 µM Cbz is depicted on Figure 8. Peak currents and peak potentials were found to vary with pH (Fig. 8A). As expected from previous works [44, 47, 76, 79], the peak potentials decreased linearly as the pH increased ($R^2 > 0.99$) (see top curve on Fig. 8B), consistent with the release of protons consecutive to Cbz oxidation. The obtained slope of -64 mV/pH suggests an equal number of electrons and protons involved in the electrochemical reaction [44, 45, 80-82]. At alkaline pH values, the observed low currents resulted from the hydrolysis of Cbz. However, too acidic media (pH < 4) should be avoided due to the the competition between protons and protonated Cbz (pKa = 4.2) for adsorption sites. The electrolytic solution pH of 5 was selected as the optimal value as it showed the best compromise in terms of signal intensity and resolution.

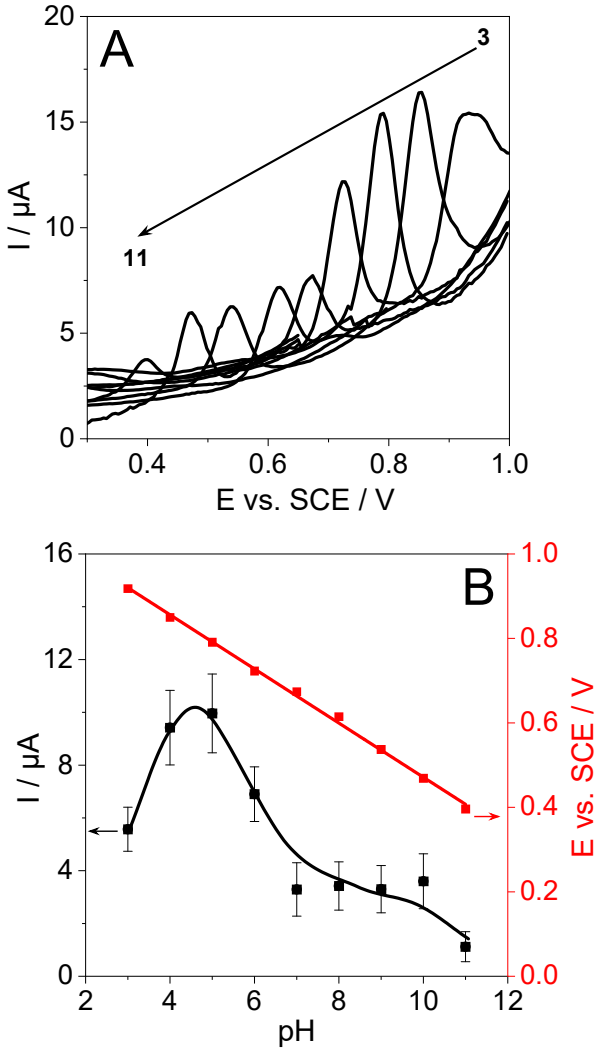

Figure 8. (A) Differential pulse voltammograms recorded in 50 µM Cbz prepared in 0.1 M phosphate buffer at various pH. (B) Variation of peak potentials (red squares) and peak currents (black circles) as function of pH (error bars correspond to n=5).

Calibration. Series of DPV curves were recorded in phosphate buffer solutions (pH 5) containing Cbz at concentrations ranging between 0.1 µM and 2.0 µM, using GCE/CNTs-MAS$_{4.8}$ as working electrode. As expected, the signal intensity increased with the concentration of Cbz in solution. Figure 9A shows the data obtained for Cbz analysis in electrolyte solution prepared from deionised water. A linear trend between the peak current and Cbz concentration ($R^2 > 0.99$) was obtained (inset of Fig. 9A), with a sensitivity of 2.61 ± 0.08 µA µM^{-1}. Based on a signal-to-noise ratio of 3, a detection limit of 0.04 µM was obtained. This value was far below the maximum allowable concentration limit of 100 ppb (0.52 µM) in water permitted by the World Health Organization [83]. Moreover, this detection limit of 0.04 µM was in the range of those reported for several Cbz electrochemical sensors [33, 44-57, 84-89], and lower than values obtained on most electrodes prepared from rather simple modifiers; the sensor was slightly less efficient compared to those based on some nanomaterials such as graphene or MXenes (see Table S1). In order to evaluate the effectiveness of GCE/CNTs-MAS$_{4.8}$ for Cbz determination in environmental samples, a calibration curve was built using spring water collected near Mendong-Yaoundé city to prepare the electrolytic solution (Fig. 9B, inset). The pH was adjusted to 5 and DPV signals recorded for Cbz added in the concentration range 0.4 µM to 2.0 µM. Excellent linearity ($R^2 > 0.99$) and sensitivity (2.71 ± 0.09 µA µM^{-1}) close to that observed in deionised water were obtained. However, due to noisier background currents, the calculated detection limit (0.08 µM) was two-fold higher, but still below the maximum allowable concentration limit of 0.52 µM.

Reproducibility. For the assessment of the repeatability, DPV response of GCE/CNTs-MAS$_{4.8}$ sensor in a 2 µM Cbz solution was recorded five consecutive times in phosphate buffer (pH 5) in the same working day at 2 h time interval. During these 2 h, the electrode was dipped in phosphate buffer (pH 5) without Cbz. A standard deviation of 5.8% was obtained, indicating a good reproducibility.

Analysis of Cbz in pesticide formulations. To demonstrate the ability of the modified electrode to determine carbendazim in real samples containing the pesticide, we have examined a commercially available pesticide formulation (grefonsec complex 210WP, with

carbendazim at 50g/Kg, as purchased from a local market). The analytical sample was prepared simply by dilution, and analysed using the standard addition method. The results are reported in Table 1. As shown, a recovery value of ca. 90% was obtained with respect to the supplier specifications, indicating good confidence level of the modified electrode.

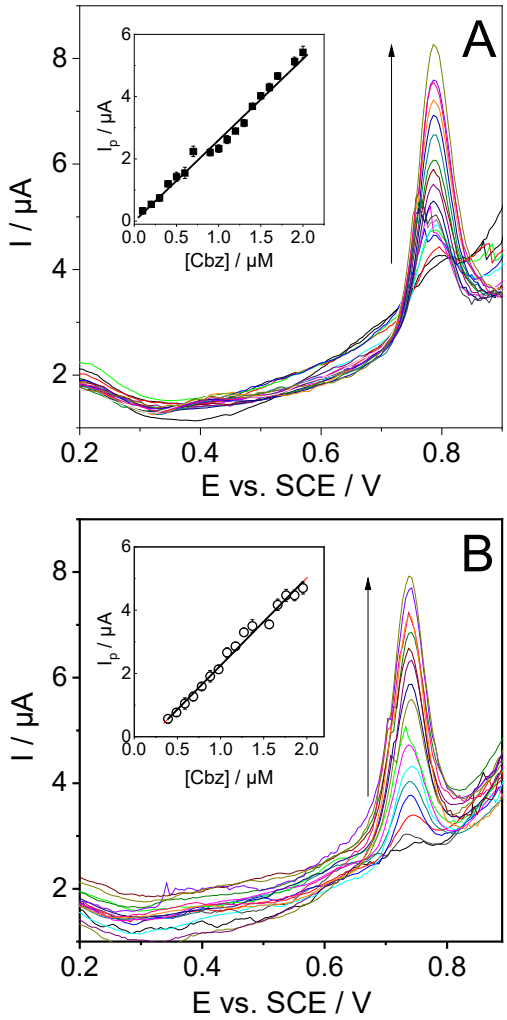

Figure 9. Differential pulse voltammograms recorded in 0.1 M phosphate buffer (pH 5) solutions prepared from (A) deionised water and (B) spring water, to which Cbz has been added at concentrations ranging from 0.1 µM to 2.0 µM. Insets: the corresponding calibration curves plotted with the mean value of three consecutive measurements.

Table 1. Determination of carbendazim in a commercial pesticide formulation using GCE/CNTs-$MAS_{4.8}$.

Sample	Stated content	Detected content	Recovery (%)
Grefonsec complex 210WP (carbendazim 50g/Kg)	0.155 mg	0.14 mg	90.3

4- Conclusion

In the present work, composite materials based on *Ayous* sawdust and CNTs have been prepared as electrode modifiers, and applied carbendazim analysis in aqueous solution. The pre-treatment of the sawdust with maleic anhydride improved its adsorption properties towards Cbz and, therefore, its electrochemical response to the pesticide. To overcome the insulating properties of the LM matrix, *Ayous* sawdust particles were dispersed in carbon nanotubes prior to deposition onto glassy carbon electrode. The resulting composite layers remain permeable to redox probes in solution, but the carboxylated surface contributed to reject anions while accumulating cations. After the optimization of the composite material formulation and the pH of the electrolyte solution, carbendazim was detected with a sensitivity of 2.61 ± 0.08 µA μM^{-1} and a detection limit of 0.04 µM.

This work has demonstrated that the formulation of a sawdust-CNTs composite material represents a promising strategy to valorize a biosourced product (*Ayous* sawdust) to build an efficient electrochemical sensor for the sensitive determination of Cbz pesticide. This could also represent an attractive way to promote the use of this renewable material as electrode modifier for other electroanalytical applications.

Acknowledgements

The authors are grateful to AUF through the grant AUF-BACGL-2014-058 and International Science Program (ISP) through the African Network of Electroanalytical Chemists (ANEC) financial grants. Dr Grégoire Herzog (Université de Lorraine, France) is thanked for facilitation in SEM analyses.

References

[1] A. J. Bard, *J. Chem. Educ.* **1983**, *4*, 302-304.

[2] J. Wang, *Electroanalysis* **1991**, *3*, 255-259.

[3] C. Mousty, *Appl. Clay Sci.* **2004**, *27*, 159-177.

[4] P. Aranda, M. Darder, R. Fernandez-Saavedra, M. Lopez-Blanco, E. Ruiz -Hitzky, *Thin Solid Films* **2006**, *495*, 104-112.

[5] C. Mousty, *Anal. Bioanal. Chem.* **2010**, *396*, 315-325.

[6] I. K. Tonle, E. Ngameni, F. M. Tchieno, A. Walcarius, *J. Solid State Electrochem.* **2015**, *19*, 1949-1973.

[7] A. Walcarius, *Chem. Soc. Rev.* **2013**, *42*, 4098-4140.

[8] A. Walcarius, *Anal Chim. Acta* **1999**, *384*, 1-16.

[9] R. W. Murray, *Ann. Rev. Mater. Sci.* **1984**, *14*, 145-169.

[10] M. A. Hubbe, S. H. Hasan, J. J. Ducoste, *BioResources* **2011**, *6*, 2161-2287.

[11] B. Esteves, L. Cruz-Lopes, A. Figueirinha, L. Teixeira de Lemos, J. Ferreira, H. Pereira, I. Domingos, *Eur. J. Wood Prod.* **2017**, *75*, 903-909.

[12] A. E. Burakov, E. V. Galunina, I. V. Burakova, A. E. Kucherova, S. Agarwal, A. G. Tkachev, V. K. Gupta, *Ecotox. Environ. Saf.* **2018**, *148*, 702-712.

[13] X. Chen, R. Xu, Y. Xu, H. Hu, S. Pan, H. Pan, *J. Hazard Mater.* **2018**, *350*, 38-45.

[14] E. Sjostrom, in *Wood chemistry: fundamentals and applications, 2nd Ed.*, Academic Press, Inc., London, **1993**, pp 12-13.

[15] H. Abdellaoui, R. Bouhfid, A. E. K. Qaiss, in *Lignocellulosic fibres reinforced thermoset composites: Preparation, characterization, mechanical and rheological properties* (Ed.: S. Kalia), Springer, Cham **2018**, pp. 215-270.

[16] A. Abdolali, W. S. Guo, H. H. Ngo, S. S. Chen, N. C. Nguyen, K. L. Tung, *Bioresour. Technol.* **2014**, *160*, 57-66.

[17] I. Švancara, A. Walcarius, K. Kalcher, K. Vytřas. *Central Eur. J. Chem.* **2009**, *7*, 598-656.

[18] S. S. Shukla, L. J. Yu, K. L. Dorris, A. Shukla, *J. Hazard Mater.* **2005**, *B121*, 243-246.

[19] S. Kong, E. T. Kamga, V. Fossog, C. P. Nanseu-Njiki, *J. Chem. Pharm. Res.* **2016**, *8*, 342-353.

[20] J. F. Fiset, J. F. Blais, R. Ben Cheikh, R. D. Tyagi, *Rev. Sci. Eau* **2000**, *13*, 325-349.

[21] L. C. K. Akissi, K. Adouby, E. N. Wandan, B. Yao, K. P. Kotchi, *J. Appl. Sci.* **2010**, *10*, 1536-1544.

[22] C. P. Nanseu-Njiki, G. K. Dedzo, E. Ngameni, *J. Hazard Mater.* **2010**, *179*, 63-71.

[23] F. T. Kamga, *Appl. Water Sci.* **2019**, *9*, 1-7.

[24] G. K. Dedzo, C. P. Nanseu-Njiki, E. Ngameni, *Talanta* **2012**, *99*, 478-486.

[25] J. R. Njimou, A. Măicăneanu, C. Indolean, C. P. Nanseu-Njiki, E. Ngameni, *Environ. Technol.* **2016**, *37*, 1369-1381.

[26] C. B. Njine-Bememba, G. Kenne Dedzo, C. P. Nanseu-Njiki, E. Ngameni, *Holzforschung* **2015**, *69*, 347-356.

[27] B. N. Ngana, P. M. T. Seumo, L. M. Sambang, G. K. Dedzo, C. P. Nanseu-Njiki, E. Ngameni, *J. Environ. Chem. Eng.* **2021**, *9*, 104984.

[28] J. Wang, *Electroanalysis* **2005**, *17*, 7-14.

[29] I. Dumitrescu, P. R. Unwin, J.V. Macpherson, *Chem. Commun.* **2009**, *45*, 6886-6901.

[30] M. Pumera, *Chem. Eur. J.* **2009**, *15*, 4970-4978.

[31] M. S. P. Shaffer, X. Fan, A. H. Windle, *Carbon* **1998**, *36*, 1603-1612.

[32] S. Singh, N. Singh, V. Kumar, S. Datta, A. B. Wani, D. Singh, K. Singh, J. Singh, *Environ. Chem. Lett.* **2016**, *14*, 317-329.

[33] J. M. Petroni, B. G. Lucca, D. K. Fogliato V. S. Ferreira, *Electroanalysis* **2016**, *28*, 1362-1369.

[34] J. S. Đorđević, V. M. Maksimović, S. B. Gadžurić, T. M. Trtić-Petrovićl, *Anal. Lett.* **2017**, *50*, 1075-1090.

[35] S. Singh, N. Singh, V. Kumar, S. Datta, A. B. Wani, D. Singh, K. Singh, J. Singh, *Environ. Chem. Lett.* **2016**, *14*, 317-329.

[36] N. Pourreza, S. Rastegarzadeh, A. Larki, *Talanta*, **2015**, *13 4*, 24-29.

[37] Z. A. Khammas, S. S. Ahmad, *Sci. J. Anal. Chem.* **2016**, *4*, 30-41.

[38] X. Qin, Y. Xu, Y. Sun, L. Zhao, L. Wang, Y. Sun, *Anal. Lett.* **2016**, *49*, 1631-1639.

[39] M. Akkbik, O. Hazer, *Anal. Lett.* **2018**, *51*, 7-23.

[40] M. Chen, Z. Zhao, X. Lan, Y. Chen, L. Zhang, R. Ji, L. Wang, *Measurement* **2015**, *73*, 313-317.

[41] L. Su, S. Wang, L. Wang, Z. Yan, H. Yi, D. Zhang, G. Shen, Y. Ma, *Spectrochim. Acta A* **2020**, *225*, 117511.

[42] L. M. Moretto, K. Kalcher (Eds.), *Environmental analysis by electrochemical sensors and biosensors*, Springer-Verlag, New York, **2014**.

[43] R. Kalvoda, *Sci. Total Environ.* **1984**, *37*, 3-7.

[44] N. G Khare, R. A. Dar, A. K Srivastava, *Electroanalysis* **2015**, *27*, 1915-1924.

[45] G. J. Arruda, F. D. Lima, C. A. L Cardoso, *J. Environ. Sci. Health B* **2016**, *51*, 534-539.

[46] Y. Dong, L. Yang, L. Zhang, *J. Agric. Food Chem.* **2017**, 65, 727-736.

[47] M. Brycht, O. Vajdle, K. Sipa, J. Robak, K Rudnicki, J. Piechocka, A. Tasić, S. Skrzypek, V. Guzsvány, *Ionics* **2018**, *24*, 923-934.

[48] T. S. H. Pham, L. Fu, P. Mahon, G. Lai, A. Yu, *Electrocatalysis*, **2016**, *7*, 411-419.

[49] Y. Yao, Y. Wen, L. Zhang, Z. Wang, H. Zhang, J. Xu, *Anal. Chim. Acta* **2014**, *831*, 38-49.

[50] Y. Hu, W. Wang, H. Li, Q.; Li, K. Niu, *Int. J. Electrochem. Sci.* **2018**, *13*, 5031-5040.

[51] X. Liao, Z. Huang, K. Huang, M. Qiu, F. Chen, Y. Zhang, Y. Wen, J. Chen, *J. Electrochem. Soc.* **2019**, *166*, B322-B327.

[52] C. Tian, S. Zhang, H. Wang, C. Chen, Z. Han, M. Chen, Y. Zhu, R. Cui, G. Zhang, *J. Electroanal. Chem.* **2019**, *847*, 113243.

[53] Y. Xie, F. Gao, X. Tu, X. Ma, Q. Xu, R. Dai, X. Huang, Y. Yu, L. Lu, *J. Electrochem. Soc.* **2019**, *166*, B1673-B1680.

[54] X. Tu, F. Gao, X. Ma, J. Zou, Y. Yu, M. Li, F. Qu, X. Huang, L. Lu, *J. Hazard. Mater.* **2020**, *396*, 122776.

[55] T. Kokulnathan, E. Ashok Kumar, T. Wang, *Microchem. J.* **2020**, *158*, 105227.

[56] S. Sekuljica, V. Guzsvany, K. Kalcher, J. Anojcic, *J. Electrochem. Soc.* **2020**, *167*, 137504.

[57] A. Ozcan, F. Hamid, A. A. Ozcan, *Talanta* **2021**, *222*, 121591.

[58] A. G. Böwing, A. Jess, *Green Chem.* **2005**, *7*, 230-235.

[59] H. Xie, A. King, I. Kilpelainen, M. Granstrom, S. Dimitris *Biomacromolecules* **2007**, *8*, 3740-3748.

[60] M. Mora-Pale, L. Meli, T. V. Doherty, R. J. Linhardt, J. S. Dordick, *Biotechnol. Bioeng.* **2011**, *108*, 1229-1245.

[61] A. M. Da Costa Lopes, K. G. João, D. F. Rubik, E. Bogel-Łukasik, L.C. Duarte, J. Andreaus, R. Bogel-Łukasik, *Bioresour. Technol.* **2013**, *142*, 198-208.

[62] X. W. Peng, J. L. Ren, R. C. Sun, *Biomacromolecules* **2010**, *11*, 3519-3524.

[63] Z. Pang, J. Chen, C. Dong, G. Yang, Y. Liu, *Bioresour. Technol.* **2013**, *128*, 813-817.

[64] M. Chen, C. Chen, C. Liu, R. Sun, *Ind. Crop. Prod.* **2013**, *46*, 380-385.

[65] Y. Zhang, H. Li, X. Li, M. E. Gibril, M. Yu, *Carbohydr. Polym.* **2014**, *99*, 126-131.

[66] K. Zhang, H. J. Choi, J. H. Kim, *J. Nanosci. Nanotechnol.* **2011**, *11*, 5446-5449.

[67] M. Granite, A. Radulescu, Y. Cohen, *Langmuir* **2012**, *28*, 11025-11031.

[68] T. Yu, J. E. Herrera, *Colloid Surf. Sci.* **2017**, *2*, 96-106.

[69] N. E. Markovich, M. M. Reboredo, M. I. Aranguren, *Eur. J. Wood Wood Prod.* **1996**, *54*, 189-193.

[70] R. Bodirlau, C. A. Teaca, *Rom. J. Phys.* **2009**, *54*, 93-104.

[71] G. G. Essoua Essoua, P. Blanchet, V. Landry, R. Beauregard, *BioResources* **2015**, *10*, 6830-6860.

[72] C. A. Teacă, R. Bodîrlău, I. Spiridon, *Cellulose Chem. Technol.* **2014**, *48*, 863-868.

[73] H. Matsuda, *Wood Sci. Technol.* **1987**, *21*, 75-88.

[74] C. E. Banks, R. R. Moore, T. J. Davies, R. G. Compton *Chem. Commun.* **2004**, 1804-1805.

[75] A. Lasia, in *Modern Aspects of Electrochemistry, Vol 32,* (Eds.: B. E. Conway, J. O. Bockris, R. E. White), Springer, Boston, **2002**, pp. 143-248.

[76] A. J. Bard, L. R. Faulkner, in *Electrochemical methods: Fundamentals and applications, 2nd Ed.*, John Wiley and Sons, Inc., **2000**, pp. 23-44.

[77] F. Marken, A. Neudeck, A. M. Bond, in *Electroanalytical Methods: Guide to experiments and applications, 2nd ed., Vol. 1 (Ed.:* Fritz Scholz), Springer, Heidelberg, **2010**, pp. 57-102.

[78] J. G. M. Yanke, G. K. Dedzo, E. Ngameni, *Electroanalysis* **2017**, *29*, 1894-1902.

[79] C. Tiana, S. Zhanga, H. Wanga, C. Chena, Z. Hana, M. Chenc, Y. Zhuc, R. Cuia, G. Zhang, *J. Electroanal. Chem.* **2019**, *847*, 113-243.

[80] P Manisankar, C Vedhi, G Selvanathan, *Bull. Electrochem.* **2004**, *20*, 81-86.

[81] X. Zhang, J. Du, D. Wu, X. Long, D. Wang, J. Xiong, W. Xiong, X. Liao *ACS Omega* **2021**, *6*, 1488-1496.

[82] E. M. Maximiano, C. A. L. Cardoso, G. J. Arruda, *Food Anal. Methods* **2020**, *13*, 119-130.

[83] WHO, Health and Safety Guide 82: Carbendazim, Geneva, 1993. Available from: http://www.inchem.org/documents/hsg/hsg/hsg82_e.htm (accessed May 16th **2020**).

[84] W. F. Ribeiro,T. M. Guimaraes Selva, I. Campelo Lopes, E. C. S. Coelho, S. G. Lemos, F. Caxico de Abreu, V. Bernardo do Nascimento, M. Ugulino de Araujo, *Anal. Methods* **2011**, *3*, 1202-1206.

[85] P. L. A. Sundari, S. P. Palaniappan, P. Manisankar, *Anal. Lett.* **2010**, *43*, 1457-1470.

[86] C. A. Razzino, L. F. Sgobbi, T. C. Canevari, J. Cancino, S. A.S. Machado, *Food Chem.* **2015**, *170*, 360-365.

[87] S. Luo,Y. Wu, H. Gou, *Ionics* **2013**, *19*, 673-680.

[88] N. T. Djimadoum, S. K. Noumbo, A. T. Kamdem, T. R Temgoua, A. D. Mvondo Zé, I. K. Tonle, *Int. J. Electrochem.* **2016**, 7839708.

[89] J. Li, Y. Chi, *Pestic. Biochem. Physiol.* **2009**, *93*, 101-104.